Coastal Engineering 138 (2018) 227–234

Contents lists available at ScienceDirect

Coastal Engineering

journal homepage: www.elsevier.com/locate/coastaleng

Nonlinear wave crest distribution on a vertical breakwater

Valentina Laface [a], Giovanni Malara [a], Ioannis A. Kougioumtzoglou [b], Alessandra Romolo [a], Felice Arena [a,*]

[a] Natural Ocean Engineering Laboratory (NOEL), "Mediterranea" University of Reggio Calabria, Loc. Feo di Vito, 89122 Reggio Calabria, Italy
[b] Department of Civil Engineering & Engineering Mechanics, Columbia University, New York, NY 10027, USA

ARTICLE INFO

Keywords:
Nonlinear wave crest
Probability distribution
Vertical wall
Compressive sensing
Harmonic wavelet

ABSTRACT

The probability distribution of the nonlinear, up to the second order, crest height on a vertical wall is determined under the assumption of finite spectral bandwidth, finite water depth and long-crested waves. The distribution is derived by relying on the Quasi-Deterministic representation of the free surface elevation on the vertical wall. The theoretical results are compared against experimental data obtained by utilizing a compressive sensing algorithm for reconstructing the free surface elevation on the wall. The reconstruction is pursued by starting from recorded wave pressure time histories obtained by utilizing a sequence of pressure transducers located at various levels. The comparison demonstrates an excellent agreement between the proposed distribution and the experimental data, while, notably, the deviation of the crest height distribution from the Rayleigh one is considerable.

1. Introduction

The probability distribution of the crest heights in a sea state is a fundamental quantity for designing any coastal structure. The first investigation on the statistical properties of ocean waves was proposed by Longuet - Higgins (1952), who proved that linear crest heights are distributed according to the Rayleigh distribution in case of narrow-band spectra. Successively, Boccotti (1989, 2000, 2014) showed that the highest waves are distributed according to a Rayleigh distribution also for finite spectral bandwidths. In real seas, waves behave nonlinearly and this implies that their wave profile is modified strongly with respect to the linear case. Indeed, nonlinearity produces sharper and larger wave crests and flatter and smaller wave troughs.

Tayfun (1980, 1986a, 1986b, 1990) and Tung and Huang (1985) investigated the statistical properties of the nonlinear crest and trough wave amplitudes in an undisturbed wave field for the case of narrow-band spectra. A more general study was proposed by Arena and Fedele (2002) who introduced a bi-parametric family of non-linear stochastic processes representing the sea surface elevation and the wave pressure fluctuation both for progressive waves and for waves interacting with structures. Specifically, the exceedance probability of the absolute maximum and of the absolute minimum was derived for narrow-band processes, up to the second order. The case of finite spectral bandwidth in undisturbed wave field was developed theoretically and validated by both experimental data and numerical simulations by Forristall et al. (2000), Prevosto et al. (2000) and Fedele and Arena (2005). Tayfun (2006) investigated the statistics of nonlinear wave crests and wave-crest groups in deep and transitional water depths, using theoretical expressions describing the statistics of nonlinear wave crests and their groups in the form of a second-order transformation of well-known results on linear waves. Fedele and Tayfun (2009) presented a second-order model for weakly nonlinear waves and developed theoretical expressions for the expected shape of very large surface displacements. Arena and Guedes Soares (2009) developed analytical solutions of the nonlinear crest and trough amplitudes in bimodal sea states. Specifically, they extended the expression developed by Fedele and Arena (2005) by modifying the distribution parameters to account for sea states with double peaked spectra. Arena and Ascanelli (2010) derived the nonlinear crest heights distribution for three dimensional waves in a finite water depth. More recently, Zhang et al. (2015a) investigated the statistical properties of long-crested nonlinear waves measured in an offshore basin, in terms of surface elevation, wave crest and trough, and wave period and Wang (2018) proposed a transformed Rayleigh distribution of trough depth for stochastic ocean waves, using as transformation model a monotonic exponential function, calibrated such that the first three moments of the transformation model equal those of the real process.

Pelinovsky et al. (2008) derived a solution for the nonlinear shallow water equation of the wave field in front of a vertical wall and determined

* Corresponding author.
E-mail addresses: valentina.laface@unirc.it (V. Laface), giovanni.malara@unirc.it (G. Malara), ikougioum@columbia.edu (I.A. Kougioumtzoglou), aromolo@unirc.it (A. Romolo), arena@unirc.it (F. Arena).

https://doi.org/10.1016/j.coastaleng.2018.04.018
Received 19 January 2018; Received in revised form 17 April 2018; Accepted 25 April 2018

the crest height as a function of the incident wave height. Then, they used this solution to determine the exceedance probability of crest and trough amplitudes on the vertical wall. They demonstrated that freak wave events can occur at the breakwaters. In such conditions, nonlinearities are more relevant and high order models could be needed (Zhang et al., 2016).

This paper addresses the problem of determining the nonlinear wave crest amplitude distributions on a vertical wall at a finite water depth. Specifically, the crest height distribution is derived within the framework of the second order Stokes' wave theory in a reflected wave field via a solution based on the method discussed by Romolo and Arena (2008) and validated by means of experimental data recorded at Natural Ocean Engineering Laboratory (NOEL) of Reggio Calabria.

2. Theoretical distribution of nonlinear crest and trough amplitude on a vertical wall

The crest height distribution is derived by considering the Quasi-Deterministic representation of the free surface displacement in a reflected wave field at the seawall. This representation was given by Boccotti (2014) for a Gaussian sea, and by Romolo and Arena (2008) by approximating the free surface to the second order in a Stokes' expansion (a similar problem was addressed via a different approach by Sun and Zhang (2017)). In this context, if we consider a very high crest occurring at point y_0 at time t_0, the first and second order components of the free surface displacement are given by the equations

$$\overline{\eta}_{1R}(y_0, t_0 + T) = \pm\frac{4h_0}{\sigma_R^2}\int_0^\infty S(\omega)\cos(\omega T)\cos^2(ky_0)d\omega, \tag{1}$$

and

$$\begin{aligned}\overline{\eta}_{2R}(y_0,t_0+T)=&-\frac{\Xi}{g}+\frac{2h_0^2}{\sigma_R^4}\int_0^\infty\int_0^\infty S(\omega_i)S(\omega_j)\cos(k_iy_0)\cos(k_jy_0)\cdot\\&\left(\left\{A_{ij_1}^-\cos\left[(k_i-k_j)y_0\right]+A_{ij_2}^-\cos\left[(k_i+k_j)y_0\right]\right\}\cos\left[(\omega_i-\omega_j)T\right]+\right.\\&\left.\left\{A_{ij_1}^+\cos\left[(k_i+k_j)y_0\right]+A_{ij_2}^+\cos\left[(k_i-k_j)y_0\right]\right\}\cos\left[(\omega_i+\omega_j)T\right]d\omega_jd\omega_i\right.\end{aligned}\tag{2}$$

where A_{ij1}^-, A_{ij2}^-, A_{ij1}^+, A_{ij2}^+ are the interaction kernels of the nonlinear free surface displacement, Ξ is a coefficient obtained by enforcing that the mean free surface displacement is zero in the time domain at any fixed point y_0 (see Appendix for their analytical formulae), $S(\omega)$ is the frequency spectrum of the incident free surface displacement, h_0 is the linear crest height which is assumed to be very large with respect to the mean wave crest amplitude (i.e. $h_0/\sigma_R \to\infty$) and σ_R^2 is the variance of free surface elevation in a reflected wave field to the first order in a Stokes' expansion.

From eq. (1) and eq. (2), if we assume that the nonlinear crest amplitude h_C occurs at $y_0 = 0$, $T = 0$, it can be expressed as

$$\begin{aligned}h_C = h_0 + 2\frac{h_0^2}{\sigma_R^4}\int_0^\infty\int_0^\infty S(\omega_i)S(\omega_j)\Big\{&-2k_i\tanh(k_id)\delta_{ij} + \left(A_{ij_1}^- + A_{ij_2}^-\right)\\&+\left(A_{ij_1}^+ + A_{ij_2}^+\right)\Big\}d\omega_jd\omega_i,\end{aligned}\tag{3}$$

where δ_{ij} is 1, for $\omega_i = \omega_j$, or 0 otherwise.

The Quasi Deterministic representation utilized in this paper is used for the free surface displacement in a Gaussian sea state in the vicinity of a very high (compared to the mean wave crest amplitude) wave crest. As a corollary of the underlying theory, Boccotti (2014), in agreement with Longuet - Higgins (1952), proved that in a Gaussian sea state, crest and trough amplitudes follow the Rayleigh distribution even for finite spectral bandwidths. Therefore, considering that the nonlinear second order crest height h_C is a quadratic function of the linear crest height h_0, its exceedance probability can be easily determined by means of the Rayleigh distribution of h_0.

According to Eq. (3), the dimensionless wave crest $\xi_{crest} = h_C/\sigma_\eta$, with σ_η being the standard deviation of the free surface displacement($\eta = \overline{\eta}_{1R} + \overline{\eta}_{2R}$), can be written as (Fedele and Arena, 2005),

$$\xi_{crest} = u\beta + \alpha(S)\beta u^2, \tag{4}$$

where $u = h_0/\sigma_\eta$ is the linear dimensionless wave crest, $\alpha(S)$ is a parameter representing the magnitude of the second order effects, and

$$\beta = \frac{\sigma_R}{\sigma_\eta}. \tag{5}$$

In Eq. (5) σ_R and σ_η are the standard deviations of the linear and the corrected up to second order free surface displacements, respectively.

Next, starting from Eq. (5), the analytical distribution $P(\xi_{crest} > \xi)$ is determined by obtaining the formal roots of the variable u from Eq. (4) and finding the conditions on u that satisfy the inequality $\xi_{crest} > \xi$. The following expression is obtained:

$$P(\xi_{crest} > \xi) = \exp\left[-\frac{1}{8\alpha^2}\left(1-\sqrt{1+\frac{4\alpha\xi}{\beta}}\right)^2\right]. \tag{6}$$

Clearly, the determination of the probability distribution (6) relies on the calculation of the parameters α and β. The former is estimated by utilizing the representation (3) in conjunction with the dimensionless amplitude (4) yielding

$$\begin{aligned}\alpha(S) = \frac{2}{\sigma_R^3}\Bigg[&-\int_0^\infty\int_0^\infty S(\omega_i)S(\omega_j)2k_i\tanh(k_id)\delta_{ij}d\omega_jd\omega_i\\&+\int_0^\infty\int_0^\infty S(\omega_i)S(\omega_j)\left[\left(A_{ij_1}^- + A_{ij_2}^-\right)+\left(A_{ij_1}^+ + A_{ij_2}^+\right)\right]d\omega_jd\omega_i\Bigg].\end{aligned}\tag{7}$$

The latter is calculated by eq. (5). For this purpose, it is seen that, given the representations of the linear and of the nonlinear free surface displacements in a random reflected wave field at a given point y^* in the time domain,

$$\eta_{R1}(y^*, t) = 2\sum_{m=1}^{M} q_m\cos(k_my^*)\cos(\omega_mt + \varepsilon_m), \tag{8}$$

and

$$\begin{aligned}\eta_{R2}(y^*,t) = \frac{1}{2}\sum_{m=1}^{M}\sum_{n=1}^{M}q_mq_n\Big(&\left\{A_{mn_1}^-\cos\left[(k_m-k_n)y^*\right]+A_{mn_2}^-\cos\left[(k_m+k_n)y^*\right]\right\}\cos[(\omega_mt+\varepsilon_m)-(\omega_nt+\varepsilon_n)]+\\&\left\{A_{mn_1}^+\cos\left[(k_m+k_n)y^*\right]+A_{mn_2}^+\cos\left[(k_m-k_n)y^*\right]\right\}\cos[(\omega_mt+\varepsilon_m)+(\omega_nt+\varepsilon_n)]+\\&\sum_{m=1}^{M}q_m^2\left[\frac{k_m}{\sinh(2k_md)}-\frac{k_m}{\tanh(2k_md)}\cos(2k_my^*)\right],\end{aligned}\tag{9}$$

$$\beta = \left\{ 4 \int_0^\infty S(\omega_i) d\omega_i \cdot \left[4 \int_0^\infty S(\omega_i) d\omega_i + \int_0^\infty \int_0^\infty S(\omega_i) S(\omega_j) \left[\left(A_{ij_1}^- + A_{ij_2}^- \right)^2 + \frac{1}{2} \left(A_{ij_1}^+ + A_{ij_2}^+ \right)^2 \right] \delta_{ij} d\omega_j d\omega_i + \right. \right.$$
$$\int_0^\infty \int_0^\infty S(\omega_i) S(\omega_j) \left[\left(A_{ij_1}^- + A_{ij_2}^- \right)^2 + \left(A_{ij_1}^+ + A_{ij_2}^+ \right)^2 + \left(A_{ii_1}^- + A_{ii_2}^- \right) \left(A_{jj_1}^- + A_{jj2}^- \right) - 2 \left(A_{ii_1}^- + A_{ii_2}^- \right) k_j \tanh(k_j d) - \right.$$
$$\left. \left. \left. 2 \left(A_{jj_1}^- + A_{jj_2}^- \right) k_i \tanh(k_i d) + 4 k_i k_j \tanh(k_i d) \tanh(k_j d) \right] (1 - \delta_{ij}) d\omega_j d\omega_i \right]^{-1} \right\}^{1/2}, \tag{10}$$

and if the wall is considered ($y^* = 0$), the parameter β is given by the equation,

where g is the acceleration due to gravity, k is the wave number and d is the water depth.

3. Parametric analysis

The probability distribution model proposed herein depends on the spectral shape, the water depth and the wave steepness. This section proposes a parametric analysis for investigating the effects of these quantities on the distribution parameters α and β and on how their variations may affect the deviation of the nonlinear crest height distribution from the Rayleigh law.

Fig. 1 shows the comparison of the probability distributions obtained by considering three different spectral shapes, all of them characterized by the same peak frequency. Specifically, Pierson-Moskowitz (Pierson and Moskowitz, 1964), mean JONSWAP (Hasselmann et al., 1973) ($\gamma = 3.3$) and narrow JONSWAP (with $\gamma = 7$) spectra are considered. The figure elucidates the fact that the spectral bandwidth has a relatively small influence on the magnitude of the deviation from the Rayleigh law. However, it is observed that the deviation increases as the spectral bandwidth is reduced.

Next, the effect of the relative water depth d/L_p is investigated, with d being the water depth at the breakwater and L_p the wave length at the breakwater depth associated with the peak spectral period T_p. Fig. 2a shows parameters α and β as a function of the relative water depth. It is seen that the parameter α decreases for increasing values of d/L_p, while β increases in shallower waters ($0.1 < d/L_p < 0.15$) and is kept almost constant at higher values. Further, it is observed that both of them tend to be almost constant for d/L_p greater than 0.3; thus, rendering their effects more relevant in intermediate water depths. The effect of this variability on the crest height distribution is shown vis-à-vis the Rayleigh distribution (Fig. 2b), thus demonstrating that at the finite water depth the deviation of the distribution from the Rayleigh one is considerable.

The same analysis is carried out by considering different wave steepness $\varepsilon = H_s/L_p$, with H_s being the significant wave height of the given sea state and L_p the wavelength associated with the peak period of the spectrum at the breakwater water depth. The results are illustrated in Fig. 3a and 3b for the parameters and the distribution, respectively. It is seen that α increases with the wave steepness because of the fact that the nonlinearities are more relevant as the wave steepness increases. The parameter β takes values less or equal than 1. Specifically, the figure shows that β exhibits an almost constant trend up to a wave steepness of 0.045. Then, it decreases. Regarding the probability distribution, larger

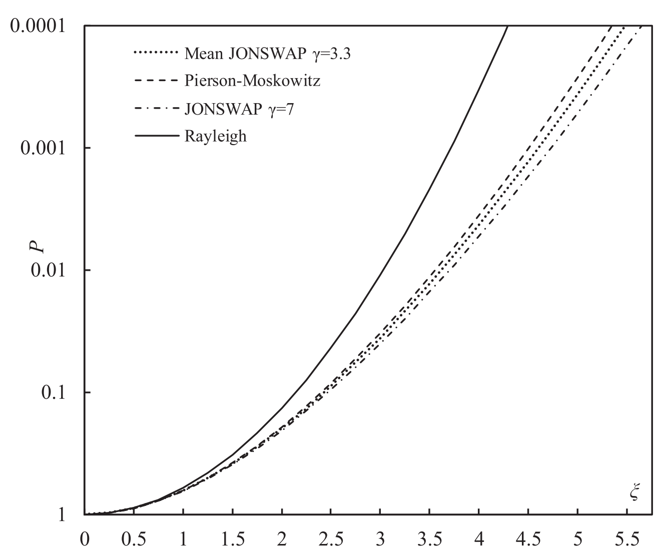

Fig. 1. Influence of the spectral bandwidth on the probability distribution.

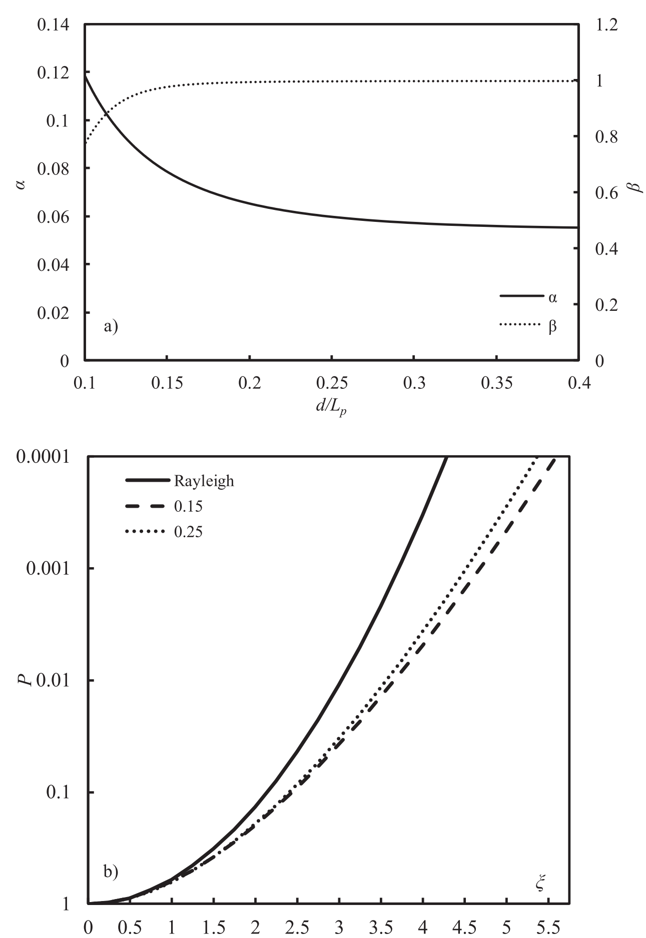

Fig. 2. a) Distribution parameters α and β as a function of relative water depth d/L_p, b) nonlinear crest height distribution for different values of d/L_p.

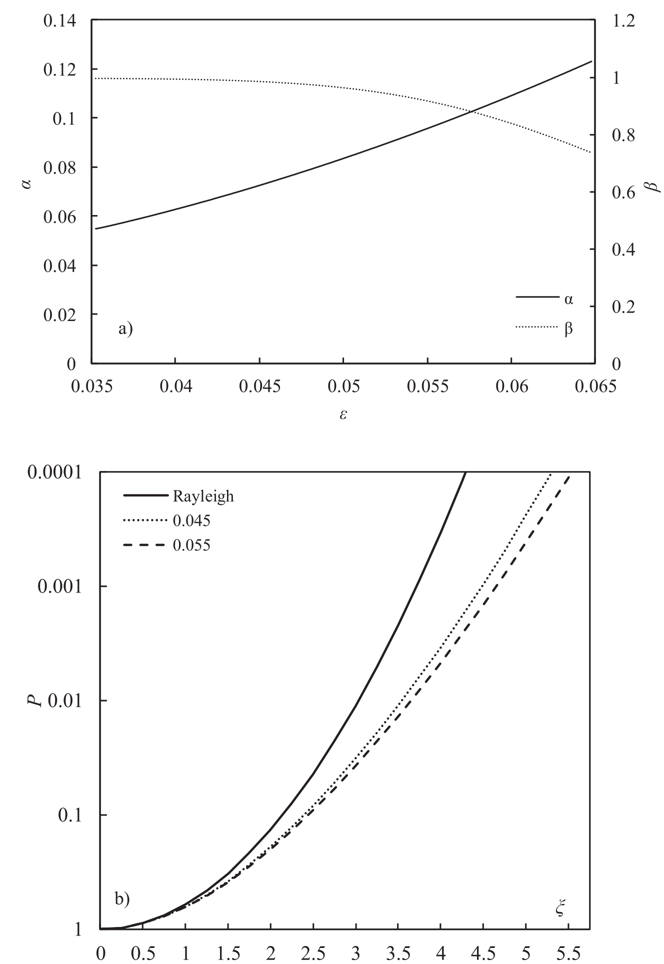

Fig. 3. a) Distribution parameters α and β as a function of wave steepness $\varepsilon = H_s/L_p$, b) nonlinear crest height distribution for different values of $\varepsilon = H_s/L_p$.

wave steepness parameters lead to a larger deviation of the crest height distribution from the Rayleigh one.

Further analysis is conducted taking into account the Ursell number U_r, defined as (Forristall et al., 2000)

$$U_r = \frac{H_s}{k_1^2 d^3}, \tag{11}$$

where k_1 is the wave number related to a frequency of $1/T_1$, with T_1 being the mean wave period calculated from the ratio of the first two moments of the wave spectrum, m_0/m_1. This parameter is used for characterizing the combined effects of water depth and of wave steepness on wave nonlinearities. The results are shown in Fig. 4a and 4b for the parameters and the distribution, respectively. The parameter α increases with U_r, while β is slightly decreasing. Fig. 4b demonstrates that an increase of the Ursell parameter leads to an increase of the deviation from the Rayleigh distribution as it has been observed considering the effects of wave steepness and the relative water depth.

4. Model validation via experimental data

Experimental data of free surface elevation on a vertical wall are used for validating the analytical distribution derived in section 2. The measurement of such a quantity is not a trivial task, because of the presence of the vertical wall, which prohibits the use of conventional ultrasonic probes. Therefore, the method proposed by Laface et al. (2018) is utilized for extrapolating indirectly the time history of the free surface

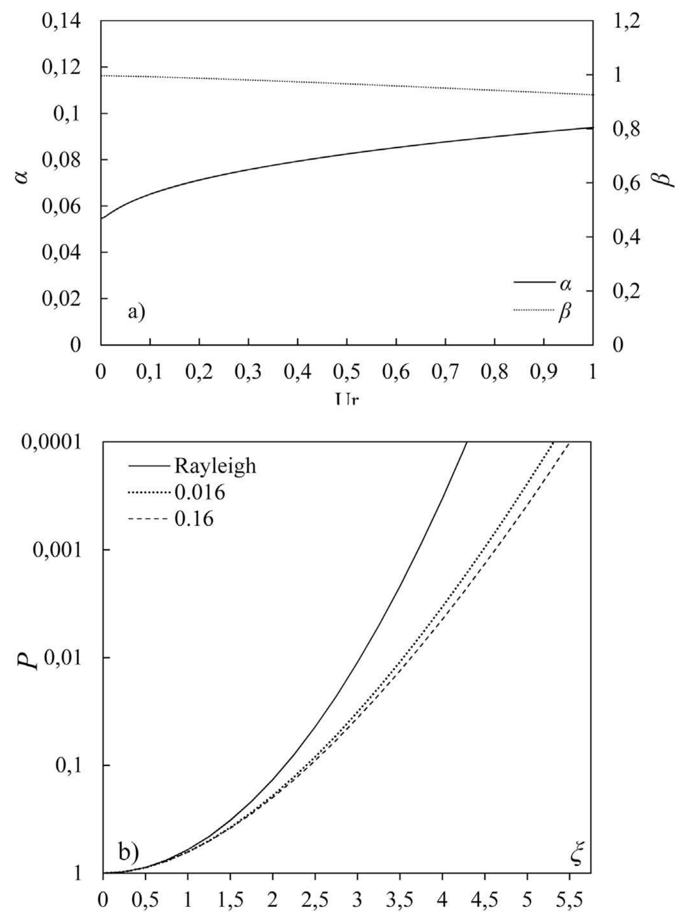

Fig. 4. a) Distribution parameters α and β as a function of Ursell number U_r, b) nonlinear crest height distribution for different values of U_r.

displacement. The method relies on the use of pressure transducers distributed on a vertical bar placed at a certain cross-section of the vertical wall (see Fig. 5a). Specifically, the approach is implemented by determining the values of the free surface displacement by observing which instruments are recording a non-zero value of the water pressure. Then, the data are processed via a harmonic wavelet based compressive sensing technique (Comerford et al., 2014, 2016, 2017; Zhang et al., 2015b; Laface et al., 2017) in conjunction with a constrained optimization problem. The main concept driving this procedure is based on the fact that the transducers under the water provide a non-zero measurement, while those above the free surface give null values. Thus, at each time instant, two kinds of information can be obtained indirectly:

1. Upper and lower bounds of the location of the instantaneous free surface;
2. Values of the instantaneous free surface at specific time instants.

The first kind of information can be achieved by analyzing two neighboring transducers, say A and B, characterized by the fact that A provides a null value and B provides a measurement different from zero at a certain time instant. In this context, the level of B is a lower bound, while the level of A is an upper bound (see Fig. 5b). The second kind of information requires analyzing two successive time instants of a pressure time history. When the sea surface crosses the transducer level, the pressure transducer gives a null value at time t and provides a certain measurement at time $t+\Delta t$ (see Fig. 5c) (and vice-versa when the free surface is moving downwards). Thus, the free surface level at time t is assumed equal to the sensor level. This approach provides an indirect measure of free surface level and therefore it may be affected by error due

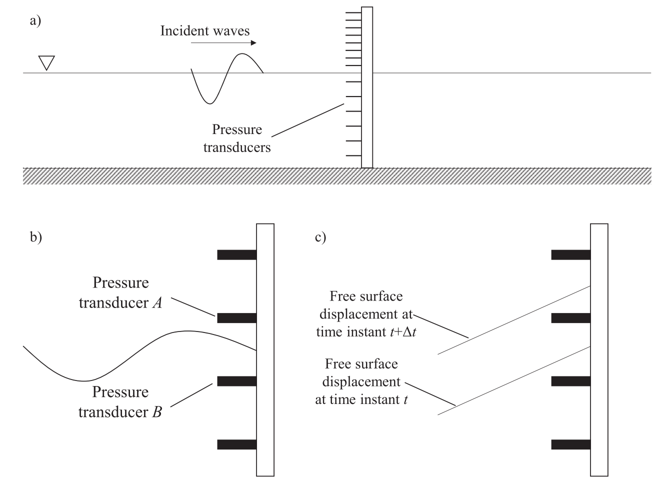

Fig. 5. a) Scheme of a vertical breakwater equipped with pressure transducers; b) scheme for identifying the upper and lower bounds of the instantaneous free surface displacement on the vertical wall; c) scheme for identifying values of the free surface at a specific time instant (free surface level is under the central pressure transducer at time t, while it is above it at time $t+\Delta t$).

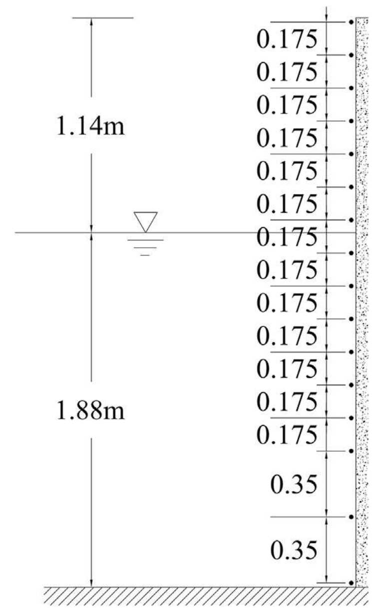

Fig. 6. Scheme of the sensors' location on the vertical breakwater.

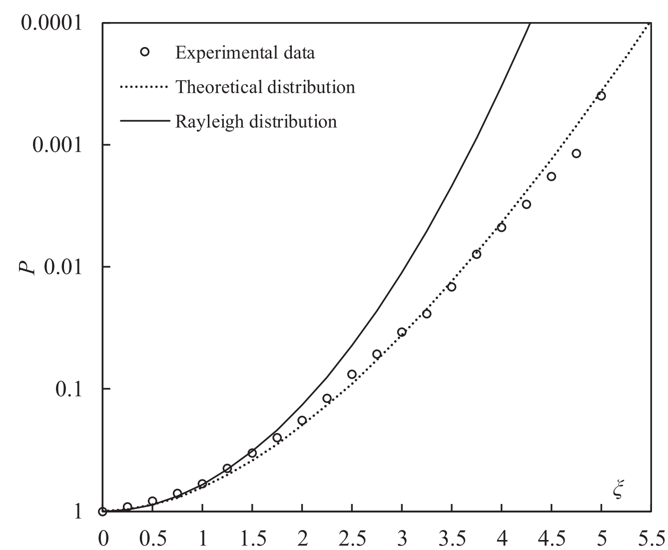

Fig. 7. Crest height distribution at seawall: comparison between theoretical results and experimental data.

to the fact that the exact time instant associated with the sensor crossing cannot be identified. However, the maximum error is of the same order of the sampling time. The free surface time history extrapolated in this manner is processed via a harmonic wavelet based compressive sensing (CS) technique (Laface et al., 2018; Comerford et al., 2016) with constraints. The classical CS that is usually implemented for a case dealing with missing data is slightly revisited by considering that the time series do not have time gaps. Instead, they have known exact values at few time instants and only upper and lower bounds in the remaining time instants. This last element requires the introduction of appropriate constraints in the associated optimization problem.

The CS method with missing data essentially consists in expanding the time history in a given basis where it is sparse and in determining the expansion coefficients by solving a system of linear equations,

$$y = Ax, \tag{12}$$

where A is the so called sampling matrix, y is the measurement vector containing the recorded values and x is the vector of the expansion coefficients to be determined. If N_0 is the original sample size and N_m the number of missing data, A is a (N_0 - N_m) by N_0 matrix, while y and x have lengths (N_0 - N_m) and N_0, respectively. According to this system (12) is underdetermined and the sparsest solution of x is obtained by an Lp–norm ($0 < p \le 1$) minimization procedure (Comerford et al., 2014; Zhang et al., 2017). The technique requires that both the signal and the sampling matrix satisfy certain properties (Candes and Wakin, 2008).

The construction of the sampling matrix A, requires the selection of an appropriate basis. Herein, the generalized harmonic wavelet (GHW) is considered (Newland, 1994). Detailed information on the methodology and the construction of A may be found in Comerford et al. (2016).

The equality constraint given by eq. (12) is considered for the N_{eq} time instants at which the exact values of the sea surface are identified. For the remaining N_{in} time instants, the upper and lower bounds constraints are expressed by means of the following inequality (Laface et al., 2018):

$$y_{\text{inf}} \le A_{in}x \le y_{\text{sup}} \tag{13}$$

where A_{in} is a N_{in} by N_0 matrix obtained from the full N_{in} by N_0 sampling matrix by removing the rows associated with the N_{eq} known values of the free surface and y_{inf} and y_{sup} are vectors of length N_{in} giving lower and upper bounds. Thus, the following constrained optimization problem arises:

$$\min_x l_1 \quad \text{such that} \begin{cases} Ax = y \\ y_{\text{inf}} \le A_{in}x \le y_{\text{sup}} \end{cases} \tag{14}$$

The experimental activity has been carried out at the Natural Ocean Engineering Laboratory of the Mediterranea University (www.noel.unirc.it). At this site the wind, blowing on a 10 km fetch, generates sea states with significant wave height H_s between 0.2 m and 1 m and with peak spectral period T_p between 2 s and 4.3 s. The data used for the analysis are pressure measurements recorded at a sampling frequency of 10 Hz. Each sea state is composed by 3 000 samples per instrument. Thus, each record has a total duration of 5 min. The sensors are placed on a vertical wall installed at a water depth of 1.8 m. Fig. 6 shows the location of the sensors on the vertical breakwater.

Given the pressure time histories on the breakwater, the approach described above is implemented for determining sea surface elevation records on the wall. Then, the crest height probability distribution is estimated from the crest data normalized with respect to the standard

Table 1
Sea state parameter ranges in the available experimental data.

H_s [m]	T_p [s]	H_s/L_p	d/L_p	U_r
0.2–0.4	1.9–2.7	0.03–0.054	0.19–0.33	0.012–0.078

deviation of the sea surface elevation of their own sea state (see Fig. 7). More precisely, the crest exceedance probability for a fixed threshold h/σ is estimated as the ratio between the number of normalized crests exceeding h/σ and the total number of waves (note that h/σ is fixed and it varies from 0 to 5.25 with a step of 0.25). The experimental dataset used for this analysis is composed by approximately 12000 waves whose significant wave height H_s in undisturbed wave field ranges between 0.2 m and 0.4 m. Table 1 shows the ranges of the recorded sea state parameters.

The parameters of the theoretical distribution are calculated by assuming that the sea waves are compatible with a mean JONSWAP spectrum (Hasselmann et al., 1973), which is the typical spectrum of the sea waves recorded at the NOEL. In this regard, considering typical wave conditions, a peak spectral frequency ω_p equal to 2.33 rad/s ($T_p = 2.7$ s) is assumed. The results of both data and theoretical distributions are shown in Fig. 7. The figure demonstrates a quite good agreement between experimental and theoretical distributions. As expected, the crest height distribution deviates from the Rayleigh distribution. Specifically, for a fixed level of exceedance probability the related dimensionless crest height is greater than that given by the Rayleigh distribution.

5. Conclusions

In this paper, an analytical crest height distribution valid in a reflected wave field has been derived and validated against experimental data. Specifically, the case of long crested waves interacting with a breakwater deployed at finite water depth has been considered.

The experimental validation has been pursued by exploiting data recorded in a natural basin and pertaining to a breakwater deployed at a certain water depth. Specifically, the free surface data on the breakwater are measured indirectly via a compressive sensing technique involving a harmonic wavelet based representation of the signal in conjunction with a constrained optimization problem. The results show an excellent agreement between the theoretical and the experimental distributions. As anticipated, the crest height distribution deviates considerably from the Rayleigh distribution, due to the crest and trough asymmetries in nonlinear seas.

Further, the effect of spectral shape, relative water depth and wave steepness on the distribution has been investigated showing that the degree of deviation from the Rayleigh law is strictly connected to those parameters.

The proposed distribution can be useful for assessing the risk associated with the occurrence of extreme waves on vertical breakwaters and has the desirable feature of incorporating into the computation spectral effects that, to the authors' knowledge, is not captured by other models available in the open literature. Further, it is emphasized that the solution is developed under the assumption of intermediate water depth and long crested random waves.

Acknowledgement

This paper was developed during the Marie Curie IRSES project "Large Multi- Purpose Platforms for Exploiting Renewable Energy in Open Seas (PLENOSE)" funded by the European Union (Grant Agreement Number: PIRSES-GA-2013-612581).

I. A. Kougioumtzoglou gratefully acknowledges the support by the CMMI Division of the National Science Foundation, USA (Award number: 1724930).

Appendix A

The coefficients $A^-_{ij\,n}$ and $A^+_{ij\,n}$ mentioned in eq. (2) are the interaction kernels of the nonlinear free surface given, respectively, by the equations,

$$A^-_{ij_n} = \frac{B^-_{ij_n}}{\omega_i\omega_j/g} + (-1)^n g\,\frac{k_i\,k_j}{\omega_i\,\omega_j} - \frac{\omega_i\,\omega_j}{g} + \frac{\omega_i^2}{g} + \frac{\omega_j^2}{g},\ n = 1,2 \tag{A.1}$$

and

$$A^+_{ij_n} = \frac{B^+_{ij_n}}{\omega_i\omega_j/g} + (-1)^n g\,\frac{k_i\,k_j}{\omega_i\,\omega_j} + \frac{\omega_i\,\omega_j}{g} + \frac{\omega_i^2}{g} + \frac{\omega_j^2}{g},\ n = 1,2 \tag{A.2}$$

where the wave frequency ω and wavenumber k are related by the linear dispersion rule

$$\omega^2 = gk\tanh(kd). \tag{A.3}$$

Moreover, the coefficients $B^-_{ij\,n}$ and $B^+_{ij\,n}$ are the interaction kernels of the nonlinear velocity potential and their solution for wave groups interacting orthogonally with the vertical wall is defined as

$$\begin{aligned} B^-_{ij_n} = {} & \frac{(\omega_i-\omega_j)\{\omega_j k_i^2[1-\tanh^2(k_i d)] - \omega_i k_j^2[1-\tanh^2(k_j d)]\}}{(\omega_i-\omega_j)^2 - g|k_i+(-1)^n k_j|\tanh[\,|k_i+(-1)^n k_j|d]} \quad n = 1,2. \\ & + \frac{2(\omega_i-\omega_j)^2 k_i\,k_j[-(-1)^n 1 + \tanh(k_i d)\tanh(k_j d)]}{(\omega_i-\omega_j)^2 - g|k_i+(-1)^n k_j|\tanh[\,|k_i+(-1)^n k_j|d]}, \end{aligned} \tag{A.4}$$

and

$$\begin{aligned} B^+_{ij_n} = {} & \frac{(\omega_i+\omega_j)\{\omega_j k_i^2[1-\tanh^2(k_i d)] + \omega_i k_j^2[1-\tanh^2(k_j d)]\}}{(\omega_i+\omega_j)^2 - g|k_i-(-1)^n k_j|\tanh[\,|k_i-(-1)^n k_j|d]} \quad n = 1,2. \\ & + \frac{2(\omega_i+\omega_j)^2 k_i\,k_j[-(-1)^n - \tanh(k_i d)\tanh(k_j d)]}{(\omega_i+\omega_j)^2 - g|k_i-(-1)^n k_j|\tanh[\,|k_i-(-1)^n k_j|d]}. \end{aligned} \tag{A.5}$$

Finally, the constant Ξ in eq. (2) is given by

$$\Xi = \frac{2gh_0^2}{\sigma_R^4}\int_0^\infty\int_0^\infty S(\omega_i)S(\omega_j)F(\omega_i,\omega_j;y_0)\mathrm{d}\omega_j\mathrm{d}\omega_i, \tag{A.6}$$

where

$$F(\omega_i,\omega_j;y_0) = \begin{cases} \cos^2(k_i y_0)\left\{-\dfrac{2k_i}{\sinh(2k_i d)} + \dfrac{2k_i}{\tanh(2k_i d)}\cdot\cos(2k_i y_0)\right\} & \text{if } \omega_i = \omega_j \\ 0 & \text{if } \omega_i \neq \omega_j \end{cases} \tag{A.7}$$

and

$$\sigma_R^2 = \sigma_R^2(y_0) = 4\int_0^\infty S(\omega)\cos^2(k\,y_0)\,\mathrm{d}\omega. \tag{A.8}$$

References

Arena, F., Ascanelli, A., 2010. Nonlinear crest height distribution in three-dimensional ocean waves. J. Offshore Mech. Arctic Eng. 132, 021604–021606.
Arena, F., Fedele, F., 2002. A family of narrow-band non-linear stochastic processes for the mechanics of sea waves. Eur. J. Mech. B Fluid 21, 125–137.
Arena, F., Guedes Soares, C., 2009. Nonlinear crest, trough, and wave height distributions in sea states with double-peaked spectra. J. Offshore Mech. Arctic Eng. 131, 1–8.
Boccotti, P., 1989. On mechanics of irregular gravity waves, Trans Nat Acc Lincei. Memorie 19, 111–170.
Boccotti, P., 2000. Wave Mechanics for Ocean Engineering. Elsevier, Amsterdam, The Netherlands.
Boccotti, P., 2014. Wave Mechanics and Wave Loads on Marine Structures. Butterworth-Heinemann, Oxford.
Candes, E.J., Wakin, M.B., 2008. An introduction to compressive sampling. IEEE Signal Process. Mag. 25, 21–30.
Comerford, L.A., Beer, M., Kougioumtzoglou, I.A., 2014. Compressive sensing based power spectrum estimation from incomplete records by utilizing an adaptive basis. In: Proceedings of the IEEE Symposium on Computational Intelligence for Engineering Solutions (CIES).
Comerford, L., Kougioumtzoglou, I.A., Beer, M., 2016. Compressive sensing based stochastic process power spectrum estimation subject to missing data. Probabilist. Eng. Mech. 44, 66–76.
Comerford, L., Jensen, H.A., Mayorga, F., Beer, M., Kougioumtzoglou, I.A., 2017. Compressive sensing with an adaptive wavelet basis for structural system response and reliability analysis under missing data. Comput. Struct. 182, 26–40.
Fedele, F., Arena, F., 2005. Weakly nonlinear statistics of high random waves. Phys. Fluids 17, 1–10.
Fedele, F., Tayfun, M.A., 2009. On nonlinear wave groups and crest statistics. J. Fluid Mech. 620, 221–239.
Forristall, G.Z., 2000. Wave Crest Distributions: Observations and Second-Order Theory. J. Phys. Oceanogr. 30, 1931–1943.
Hasselmann, K., Barnett, T.P., Bouws, E., Carlson, H., Cartwright, D.E., Eake, K., et al., 1973. Measurements of wind-wave growth and swell decay during the joint North Sea wave project (JONSWAP). Dtsch. Hydrogr. Z. A8, 1–95.
Laface, V., Kougioumtzoglou, I.A., Malara, G., Arena, F., 2017. Efficient processing of water wave records via compressive sensing and joint time-frequency analysis via harmonic wavelets. Appl. Ocean Res. 69, 1–9.
Laface, V., Malara, G., Romolo, A., Arena, F., Kougioumtzoglou, I.A., 2018. Compressive sensing based reconstruction of the sea free surface elevation on a vertical wall. J. Waterw. Port, Coast. Ocean Eng. Accepted for publication.
Longuet - Higgins, M.S., 1952. On the statistical distribution of the heights of sea waves. J. Mar. Res. 11, 245–266.
Newland, D.E., 1994. Harmonic and musical wavelets. Proc. R. Soc. Lond. Ser. A 444, 605–620.
Pelinovsky, E., Kharif, C., Talipova, T., 2008. Large-amplitude long wave interaction with a vertical wall. Eur. J. Mech. B Fluid 27, 409–418.
Pierson, W.J., Moskowitz, L., 1964. A proposed spectral form for fully developed wind seas based on the similarity theory of S. A. Kitaigorodskii. J. Geophys. Res. 69, 5181–5190.
Prevosto, M., Krogstad, H.E., Robin, A., 2000. Probability distributions for maximum wave and crest heights. Coast Eng. 40, 329–360.
Romolo, A., Arena, F., 2008. Mechanics of nonlinear random wave groups interacting with a vertical wall. Phys. Fluids 20, 036604.
Sun, Y., Zhang, X., 2017. A second order analytical solution of focused wave group interacting with a vertical wall. Int. J. Nav. Architect. Ocean. Eng. 9, 160–176.
Tayfun, M.A., 1980. Narrow-band nonlinear sea waves. J. Geophys. Res.: Oceans 85, 1548–1552.
Tayfun, M.A., 1986. On narrow-band representation of ocean waves: 1. Theory. J. Geophys. Res.: Oceans 91, 7743–7752.
Tayfun, M.A., 1986. On narrow-band representation of ocean waves: 2. Simulations. J. Geophys. Res.: Oceans 91, 7753–7759.
Tayfun, M.A., 1990. Distribution of large wave heights. J. Waterw. Port, Coast. Ocean Eng. 116, 686–707.
Tayfun, A.M., 2006. Statistics of nonlinear wave crests and groups. Ocean. Eng. 33, 1589–1622.
Tung, C.C., Huang, N.E., 1985. Peak and trough distributions of nonlinear waves. Ocean. Eng. 12, 201–209.
Wang, Y., 2018. Transformed Rayleigh distribution of trough depths for stochastic ocean waves. Coast Eng. 133, 106–112.
Zhang, H.D., Guedes Soares, C., Onorato, M., 2015. Modelling of the spatial evolution of extreme laboratory wave crest and trough heights with the NLS-type equations. Appl. Ocean Res. 52, 140–150.
Zhang, Y., Comerford, L., Beer, M., Kougioumtzoglou, I., 2015. Compressive sensing for power spectrum estimation of multi-dimensional processes under missing data. In: Proceedings of the 2015 International Conference on Systems, Signals and Image Processing (IWSSIP).
Zhang, H.D., Guedes Soares, C., Chalikov, D., Toffoli, A., 2016. Modeling the spatial evolutions of nonlinear unidirectional surface gravity waves with fully nonlinear numerical method. Ocean. Eng. 125, 60–69.
Zhang, Y., Comerford, L., Kougioumtzoglou, I., Beer, M., 2017. Lp-norm minimization for stochastic process power spectrum estimation subject to incomple data. Mech. Syst. Signal Process. 101, 361–376.

Nomenclature

α, β: = parameters of nonlinear crest height distribution
γ =: peak shape parameter of the JONSWAP spectrum
ε =: wave steepness
ε_m: = random phases
η =: free surface displacement of reflected wave field corrected up to the second order
$\overline{\eta}_{1R}$: = linear component of Quasi-Deterministic free surface elevation in a reflected wave field at the seawall
η_{R1}: = linear free surface displacements in a random reflected wave field
$\overline{\eta}_{2R}$: = second order component of Quasi-Deterministic free surface elevation in a reflected wave field at the seawall
η_{R2}: = second order free surface displacements in a random reflected wave field
ξ_{crest} =: dimensionless wave crest
σ_η^2: = variance of corrected up to second order free surface displacement of reflected wave field
σ_R^2: = variance of linear component of sea surface of reflected wave field
ω =: angular frequency
ω_p =: peak spectral frequency
Δt =: sampling rate
A: = sampling matrix
A_{in} =: reduced sampling matric
$A^-_{ij_1}$, $A^-_{ij_2}$, $A^+_{ij_1}$, $A^+_{ij_2}$: interaction kernels of the nonlinear free surface displacement
$B^-_{ij_1}$, $B^-_{ij_2}$, $B^+_{ij_1}$, $B^+_{ij_2}$: interaction kernels of the nonlinear velocity potential
d =: the water depth
g =: acceleration due to gravity
h_0 =: linear crest height of reflected wave field
h_C =: nonlinear second order crest height
H_s =: significant wave height
k =: wave number

k_1 =: wave number related to T_1
N_0 =: sample size
N_{eq} =: number of known values of the free surface surface
N_{in} =: number of bounds identified for reconstructing the free surface
N_m =: number of missing data
q_m: =wave amplitudes
$S(\omega)$ =: frequency spectrum of the incident free surface displacement
T, t =: time variables
t_0: =time instant at which the high crest height h_0 occurs
T_1 =: mean wave period
T_p =: peak spectral period
$u = h_0/\sigma_\eta$: =linear dimensionless wave crest
U_r =: Ursell number
x: =expansion coefficients vector
y: =measurements vector
y_0: =point at which the high crest height h_0 occurs
y_{inf}, y_{sup} =: vectors of length N_{in} giving lower and upper bounds of the sea surface